The exudophore, a distinct exudate-producing structure of *Pleurotus ostreatus*, carries an oxidative and secretory transcriptional signature

Richard Barker[1*], Ana Sofia Leiva[1], Manisha Dagar[1], Ayma Rizwan[1], Tayla Koenig[1], Adriana Kaley Sanchez[1], Simone X. Moulton[1], Marshall Porterfield[1]

[1][AUTHORS: affiliation].

*Corresponding author(s). E-mail(s): [AUTHORS: corresponding email];

Abstract

Filamentous fungal colonies differentiate into regions with distinct physiology, but the molecular basis of that differentiation is rarely resolved in cultivated basidiomycetes. Growing *Pleurotus ostreatus* cv. "Harbor Blue P01" in a mycoponic ceramic-tube system, we identified a discrete exudate-producing structure, here termed the *exudophore*, alongside exuding mycelium, aerial (fuzzy) mycelium and mycelial nodules. Comparative 3′-tag transcriptome profiling, analysed under criteria designed to be robust at low replicate number, shows that the exudophore carries the most reproducible tissue signature of the four: 37 of its top 50 specificity-ranked markers are supported by every biological replicate, and four co-expression modules associate with it after correction for multiple testing and for ribosomal RNA content. The signature is coherently oxidative and secretory, comprising alcohol oxidase, an FAD-dependent monooxygenase, cytochrome P450, aldehyde and formate dehydrogenases, an AA9 lytic polysaccharide monooxygenase, multiple transporters, and cyanate and cyanide hydratases. Alcohol oxidase generates extracellular hydrogen peroxide, the co-substrate required by fungal peroxidases, placing the exudophore within the oxidative enzymology characteristic of white-rot decay. Mycelial nodules, by contrast, express cerato-platanin family proteins and small heat-shock proteins consistent with fruiting-body primordium formation. We interpret these data as defining the exudophore as a transcriptionally distinct structure and propose specific, testable hypotheses about its function.

Keywords: *Pleurotus ostreatus*, exudate, fungal differentiation, alcohol oxidase, lytic polysaccharide monooxygenase, mycoponics

DRAFT — AWAITING AUTHOR INPUT

This manuscript cannot be completed without material only the authors hold: the morphological description of the exudophore, how it is distinguished from exuding mycelium, and the sampling protocol. Those points are marked [**AUTHORS**] and are load-bearing for the central claim, since the transcriptional argument rests on the structure being distinguishable in the first place. All quantitative results are generated from the analysis repository and verified by `scripts/32_audit_numbers.py`. Methodological detail is given in the companion resource paper.

1 Introduction

Filamentous fungi grow as colonies that are physiologically heterogeneous. Regions of the same mycelium differ in age, in nutrient access, in the enzymes they secrete and in their developmental trajectory, and this heterogeneity is functionally important: it underlies foraging, substrate decay and the transition to fruiting. Yet in cultivated basidiomycetes the molecular basis of regional differentiation is rarely resolved, in part because sampling discrete structures from a colony is difficult in conventional solid-substrate culture.

Guttation—the exudation of liquid droplets from mycelium—is a widespread and long-observed fungal phenomenon whose function remains debated. Exudates have been variously proposed to serve osmotic regulation, excretion of metabolic by-products, extracellular enzyme deployment, and secondary-metabolite storage. Distinguishing among these possibilities requires knowing which cells produce the droplets and what those cells are transcribing.

[**AUTHORS: two paragraphs required here.**] The first should describe the exudophore morphologically: what it looks like, at what scale, how it is distinguished from exuding mycelium, when it appears during culture, and whether comparable structures have been described previously in *Pleurotus* or other genera. The second should state the hypothesis being tested. Without the first, the central claim of this manuscript—that the exudophore is a distinct structure—rests on transcriptional evidence alone, which is weaker than it needs to be.

The mycoponic culture system used here [1] grows mycelium on micro-structured ceramic tubes supplied with liquid nutrient medium through a size-exclusion interface. Because the mycelium develops on an accessible surface rather than through an opaque substrate, discrete structures can be identified and sampled individually. We used this to compare four tissue types by 3′-tag transcriptome profiling.

2 Results

2.1 Two of four tissues yield reproducible signatures

Transcriptomes were obtained for four tissues with four biological replicates each. The sequencing yielded a low fraction of usable mRNA (analysed in detail in the companion resource paper), so all conclusions here are drawn under criteria chosen to be robust at low replicate number, and four libraries falling below a pre-specified count threshold were excluded.

Tissue specificity was scored with the τ index. Because τ is computed on tissue means, a single outlying replicate can manufacture an apparent marker, so we additionally required that *every* replicate of a tissue exceed the maximum value observed in any sample of any other tissue. Of the top 50 markers per tissue, this was satisfied by 37 for the exudophore and 22 for the nodule, but by only 1 each for exuding and fuzzy mycelium. Independently, weighted gene co-expression network analysis produced 41 modules, of which six showed a tissue association surviving Benjamini–Hochberg correction across all 168 module $\times$ tissue tests—four associated with the exudophore and two with the nodule, and none with either mycelial tissue (Fig. 2a).

That two methods sensitive to different failure modes converge on the same two tissues is the basis for restricting interpretation to the exudophore and the nodule. The absence of a signature for exuding and fuzzy mycelium reflects the resolving power of these libraries and should not be read as an absence of distinct biology in those tissues.

2.2 The exudophore signature is oxidative and secretory

Among the 37 replicate-supported exudophore markers, 24 have a characterised homologue. They fall into four functional groups.

Oxidative enzymes. Alcohol oxidase 1 (EC 1.1.3.13), an FAD-dependent monooxygenase, cytochrome P450 monooxygenase, aldehyde dehydrogenase (EC 1.2.1.3), formate dehydrogenase (EC 1.17.1.9) and peroxisomal catalase (Fig. 1). Alcohol oxidase is notable: it generates hydrogen peroxide extracellularly, and H_2O_2 is the obligatory co-substrate of the class II peroxidases that mediate white-rot lignin attack. Aldehyde and formate dehydrogenases together constitute a route for oxidising aldehydes to CO_2, consistent with handling reactive carbonyl products.

Carbohydrate-active enzymes. An AA9 family lytic polysaccharide monooxygenase (EC 1.14.99.54), a copper enzyme that oxidatively cleaves crystalline cellulose and itself requires an external electron donor and oxygen.

Transport. An MFS-type transporter, an uncharacterised transporter and an amino-acid permease, consistent with substantial solute movement across the plasma membrane.

Detoxification. Cyanate hydratase (EC 4.2.1.104) and cyanide hydratase (EC 4.2.1.66). Cyanide hydratase is characteristic of fungi that tolerate cyanogenic substrates; its enrichment in an exudate-producing structure is unexpected and, in our view, the single most interesting hypothesis-generating observation in these data.

All 16 replicate-supported markers with a characterised homologue show the same pattern: elevated in both exudophore replicates and unremarkable in all ten libraries of the other three tissues (Fig. 1).

The four exudophore-associated co-expression modules are consistent with this picture and add a growth dimension: the most strongly associated module ($r = +0.91$) enriches for small-subunit rRNA maturation, a ribosome-biogenesis signature. Because these libraries carry a high and variable ribosomal RNA content, we tested this explicitly and found the module eigengene correlates with per-library rRNA fraction at only -0.15; the tissue association is unchanged when computed as a partial correlation controlling for it (Fig. 2b). The exudophore therefore appears to be a metabolically active, high-biosynthesis structure rather than a passive site of leakage.

2.3 Nodules express a fruiting-body primordium signature

The nodule-associated module ($r = +0.85$, 320 genes) enriches for extracellular space and for oxidoreductases acting on CH-OH groups, and contains 22 predicted secreted proteins and 11 carbohydrate-active enzymes. It also enriches for the term "protein aggregate centre". The replicate-supported nodule markers are independently dominated by cerato-platanin family proteins and small heat-shock proteins. Cerato-platanins are small secreted cysteine-rich proteins associated with fungal development and with fruiting-body formation; small heat-shock proteins prevent protein aggregation, which the module-level enrichment recovers by a wholly different route. Together these support interpretation of the nodule as an early fruiting-body primordium.

2.4 Pairwise contrasts

The strongest contrast in the dataset is nodule against exudophore (198 genes at $p_{\mathrm{adj}} < 0.05$, $|\log_2 \mathrm{FC}| > 1$), followed by fuzzy mycelium against exudophore (50) and exudophore against exuding mycelium (36). Fuzzy mycelium against exuding mycelium yields essentially none, reproducibly and across two independent reference genomes, which is consistent with these being two presentations of vegetative mycelium rather than distinct differentiated states.

3 Discussion

[**AUTHORS: this section needs the morphological context to be written properly.**] The transcriptional argument is complete, but its interpretation depends on what the exudophore is structurally. The following points are supported by the data as they stand.

An oxidative, H_2O_2-generating signature in an exudate-producing structure suggests a functional link between guttation and extracellular oxidative chemistry. Alcohol oxidase and an AA9 lytic polysaccharide monooxygenase both operate extracellularly and both depend on oxygen; the LPMO additionally requires an electron donor. A liquid droplet is a plausible medium in which such chemistry could be organised, and the co-enrichment of transporters is consistent with active loading rather than passive leakage. This suggests a testable prediction: exudate droplets should contain H_2O_2 and oxidoreductase activity, which is directly measurable.

Cyanide and cyanate hydratase enrichment is unexplained and worth pursuing. Neither the medium nor the substrate is obviously cyanogenic. Possible explanations include a constitutive detoxification capacity, a response to a medium component, or a role for these enzymes in nitrogen metabolism, cyanate being a substrate for carbamoyl phosphate turnover.

The ribosome-biogenesis association argues against a degenerative interpretation. Exudation is sometimes framed as excretion or as an artefact of senescence. A structure whose most strongly associated co-expression module concerns ribosome biogenesis is more consistent with active growth.

3.1 Limitations

Two of four tissues could not be characterised at the depth achieved, and the exudophore result rests on two libraries after quality filtering. The functional annotation covers 41% of the proteome, and lineage-specific secreted proteins—the class most likely to be relevant to a novel structure—are systematically the least likely to be annotated, so the signature described here is probably incomplete in a biased direction. All functional assignments are inferred from homology; none has been tested experimentally in this organism. The proposed links between the transcriptional signature and exudate function are hypotheses, not conclusions.

4 Methods

Culture, sequencing, read processing, annotation and statistical analysis are described in full in the companion resource paper, and all code and intermediate results are available in the accompanying repository. In brief: four tissue types with four biological replicates were profiled by poly(A)-selected 3′-end tag sequencing; reads were aligned to *P. ostreatus* BOM_ss5 (`GCA_056149245.1`) with an rRNA-complete, 3′-extended annotation; counts were normalised with DESeq2 [2] after excluding libraries below 15,000 assigned non-rRNA counts; co-expression modules were derived with WGCNA [3] and corrected with Benjamini–Hochberg [4]; specificity was scored with the τ index [5] on linear normalised counts.

[AUTHORS: sampling procedure, tissue definitions and the morphological basis for distinguishing the exudophore from exuding mycelium; RNA extraction method; culture age at sampling.]

Figures

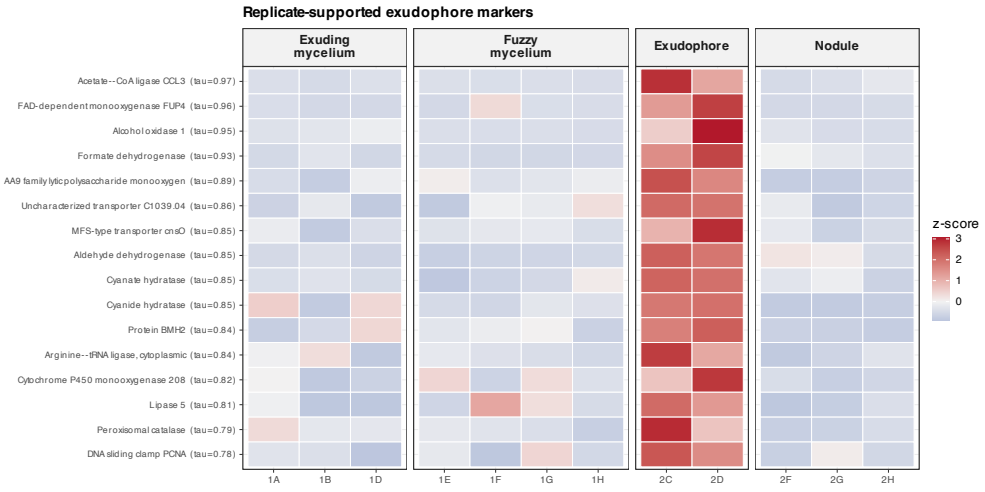


Fig. 1 The exudophore signature is reproducible across replicates. Row-scaled expression of the replicate-supported exudophore markers carrying a characterised homologue, across all 12 retained libraries. Each marker is elevated in both exudophore replicates and unremarkable elsewhere; this is the criterion by which they were selected, and the figure shows the margin by which it is met. τ, tissue-specificity index.

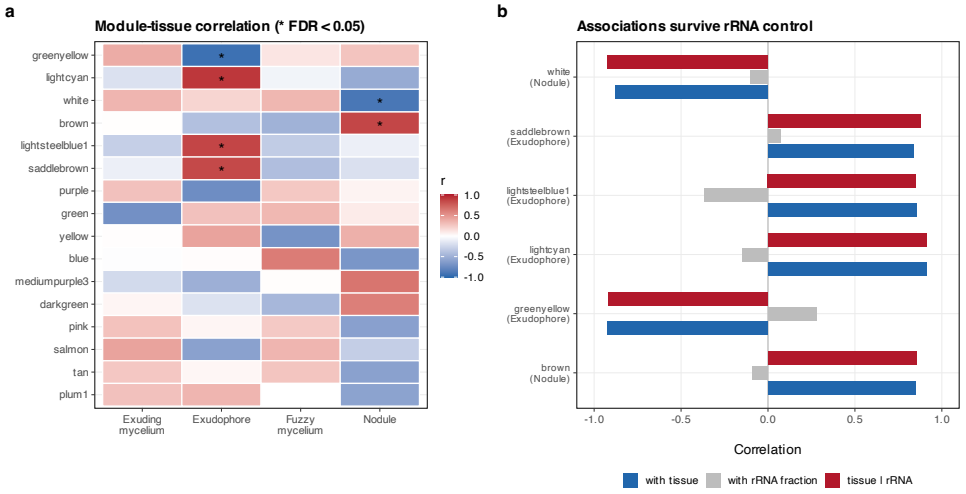


Fig. 2 Co-expression modules corroborate the marker analysis. a, Module–tissue correlation; asterisks mark associations surviving Benjamini–Hochberg correction across all 168 tests. Only exudophore and nodule have surviving modules. **b**, Each surviving association compared with its correlation to per-library ribosomal RNA fraction, and recomputed as a partial correlation controlling for it. All six survive, including the exudophore ribosome-biogenesis module.

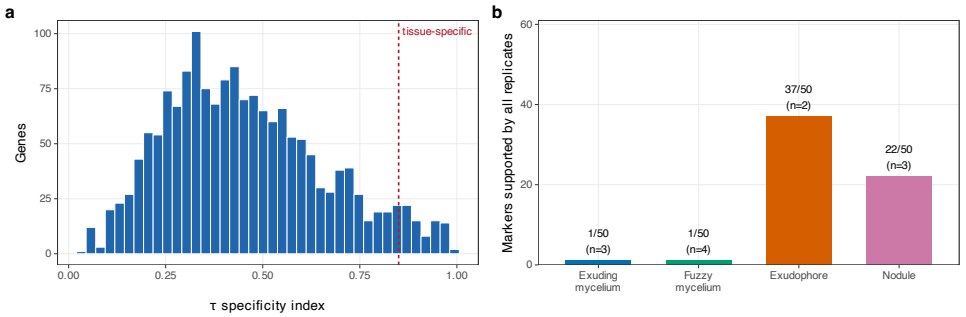


Fig. 3 Specificity scores and replicate support by tissue. a, Distribution of the τ specificity index across all scored genes. **b**, Of the top 50 markers per tissue, the number supported by every biological replicate. The test becomes more stringent as replicate number rises, so counts are not directly comparable across tissues.

Tables

Table 1 Differential expression across all six pairwise contrasts (12 retained libraries, rRNA-removed track; $p_{\mathrm{adj}} < 0.05$, $|\log_2 \mathrm{FC}| > 1$).

Tissue A	Tissue B	DE genes
Nodule	Fuzzy mycelium	239
Nodule	Exudophore	198
Nodule	Exuding mycelium	74
Fuzzy mycelium	Exudophore	50
Exudophore	Exuding mycelium	36
Fuzzy mycelium	Exuding mycelium	2

Data availability. https://github.com/dr-richard-barker/Myco_tissue_RNAseq. Raw reads: SRA accession pending. Companion resource paper describes the pipeline, corrected annotation and metabolic reconstruction in full.

Author contributions. [AUTHORS: CRediT statement for all eight authors.]

Funding. [AUTHORS.]

Competing interests. [AUTHORS: declaration.]

References

[1] Porterfield, D. M. *et al.* Mycoponics: Controlled bioproduction utilizing biophysical, solid-state, liquid nutrient delivery. *Biotechnology Journal* **21** (2026).

[2] Love, M. I., Huber, W. & Anders, S. Moderated estimation of fold change and dispersion for rna-seq data with deseq2. *Genome Biology* **15**, 550 (2014).

[3] Langfelder, P. & Horvath, S. Wgcna: an r package for weighted correlation network analysis. *BMC Bioinformatics* **9**, 559 (2008).

[4] Benjamini, Y. & Hochberg, Y. Controlling the false discovery rate: a practical and powerful approach to multiple testing. *Journal of the Royal Statistical Society: Series B* **57**, 289–300 (1995).

[5] Yanai, I., Benjamin, H., Shmoish, M. *et al.* Genome-wide midrange transcription profiles reveal expression level relationships in human tissue specification. *Bioinformatics* **21**, 650–659 (2005).